Memoirs of the Faculty of Engineering, Kyushu University, Vol. 74, No. 2, September 2014

Rockfall Hazard Assessment in Gunung Kelir Area Yogyakarta, Indonesia

by

Guruh SAMODRA[*], Guangqi CHEN[**] , Junun SARTOHADI [***]
and Kiyonobu KASAMA[†]

(Received July 23, 2014)

Abstract

Rockfall hazard assessment should be treated in a different way compared to other mass wasting phenomena due its complex nature. Rockfall hazard assessment involves determination of rockfall source, size-frequency, onset susceptibility, temporal probability and deposit area. In this paper, we propose a methodological framework of rockfall hazard assessment which is expected to answer "where", “how frequent” and “how large” rockfall are likely to occur. Rockfall inventory and frequency-size analysis are employed to assess temporal distribution, size and frequency of rockfall which may occur in the future. GIS-lumped mass rockfall simulation is employed to identify potential rockfall source based on the distribution of boulders from the past rockfall events. And then, reliable trajectories are estimated once the potential rockfall sources are identified. It represents the rockfall susceptibility degree in the study area. Since GIS-lumped mass model does not consider the size, shape and fragmentation of the boulder, 2D DDA is employed to analyze the trajectory which has a potency of high risk, e.g. trajectory passing a building. Information of rockfall hazard represented as the susceptible location and magnitude-frequency, including temporal probability of rockfall can be further employed to formulate an appropriate landuse planning in a rockfall prone area.

Keywords: Rockfall, Hazard, GIS, DDA, Frequency-magnitude

1. Introduction

The word rockfall is often distinguished from more general landslide phenomena due its typical material, size and failure mechanism. It is defined as rock fragments[1)] with size from a few dm^3 to 10^4 m^3 [2)] started by the detachment of blocks from their original position[3)] and followed by free falling, bouncing, rolling or sliding [4)]. As a consequence, determining rockfall hazard will not be simple to achieve in practice[3)] due to its complex nature. Rockfall hazard assessment involves determination of rockfall source, size-frequency, spatial probability/onset susceptibility, intensity, and deposit area.

[*] Graduate Student, Department of Civil and Structural Engineering
[**] Professor, Department of Civil and Structural Engineering
[***] Professor, Department of Environmental Geography Universitas Gadjah Mada
[†] Associate Professor, Department of Civil and Structural Engineering

Identification of potential rockfall source in medium to large scale mapping is one of the main difficulties in rockfall hazard assessment[5]. Several authors have proposed simple empirical threshold angles for potential rockfall source such as slope >45°[6], slope >60°[7] and slope >37°[8]. Recent methods are by combining several parameters such as slope angle, discontinuity, curvature, slope scree, distance to fault, block size[9], geology and rock condition, slope, ditch dimension, seepage, event history[10]; by using DEM-based geomorphometric analysis[5]; and by employing terrestrial laser scanner[11].

Size-frequency is usually based on the rockfall inventory data. However, complete inventory data are not available in many developing countries. Most complete inventory data are available in developed country e.g. Grenoble French Alps, French[2], Yosemite California, USA[12,7] and British Columbia, Canada [13]. Several laws for frequency-magnitude of rockfall have been successfully proposed by Hungr et al.[13] and Dussauge et al.[14] because of the availability of complete historical data. However, the major limitations to size-frequency analysis include the lack of rockfall inventories for most sites and the spatial and temporal heterogeneity of available inventories.

Rockfall spatial probability/onset susceptibility employed several approaches such as GIS (Geographic Information System) susceptibility mapping, numerical simulations and full scale experiment[15]. The application of rockfall susceptibility assessment usually depends on the scale of the area. GIS susceptibility mapping is usually applied in regional scale, whereas numerical simulations and full scale experiment are applied in a limited area or large scale. Most spatial probability approaches include intensity analysis, i.e. velocity and energy.

GIS susceptibility mapping is a powerful tool to assess spatial probability of rockfall in regional scale (large area). It is based on Digital Terrain Model (DTM) representing topography in raster format. The model is very powerful to simulate the physical characteristics of the surface rather than the physical characteristic of the boulder itself. The additional attribute related to geology, land use or vegetation type and rock type represented in spatial data can also be included in the model. GIS model is able to determine the trajectory of rockfall movement, the deposit area and the potential intensity of rockfall. However, GIS models usually use lumped mass approach[16]. It means that the boulder of rockfall is dimensionless; without considering the size, shape and mass of the boulder.

Numerical rockfall simulation such as DDA[17] is able to represent rockfall more realistic. The contact forces are calculated during the interaction between boulder and slope. Modeling the dynamic displacement and deformation of an elastic body in any shape are the advantages of the DDA. It includes the rigid body displacement, rotation and deformation of a block. Reliable trajectory and dynamic behavior of boulder when travel along the slope are also able to be identified based on the characteristic of material, shape and size. However, DDA simulation will be more complex, need excessive computational requirements[16] and time consuming when it is applied in large area or regional scale.

Rockfall threat in Gunung Kelir is one of the main concerns in Kulon Progo local government. Several rock fragments fell down through the colluvial foot slope and[18]. PSBA UGM[19] conducted a preliminary qualitative hazard assessment to provide guidance on the design of rockfall measures for the local government. It involves expert judgement on the potential occurrence of rockfall hazard based on geomorphological survey and the position of element at risk. The qualitative hazard assessment was the only possible approach employed at that time due to the limited time and the absence of available rockfall data.

This paper is aimed to propose an additional hazard analysis for better understanding of rockfall hazard containing susceptibility, size-frequency and temporal probability. It involves frequency-volumes statistics of rockfall deposits inventory, spatial trajectories of potential rockfall

and simulating physical mechanism of rockfall displacement and deformation in the trajectory which has a potency of high risk. In addition, impact force analysis is also performed to infer the physical vulnerability of element at risk in a specific scenario.

2. Study Area

Gunung Kelir is located in the western part of Yogyakarta Province, Indonesia (**Fig. 1**). It lies in the upper part of Menoreh Dome that is located in central part of Java Island. The area is dominated by Tertiary Miocene Jonggrangan Formation that consists of calcareous sandstone and limestone. Bedded limestone and coralline limestone which form isolated conical hills may also be found in the highest area surrounding study area. Weathering, erosion, and mass movement are common geomorphological processes in the study area. *Gunung* (Mountain) *Kelir*, of Javanese origin, literally means a curtain that is used to perform *wayang* (Javanese traditional puppet). Its toponym describes a 100-200 meter high escarpment that has slope nearly 90°.

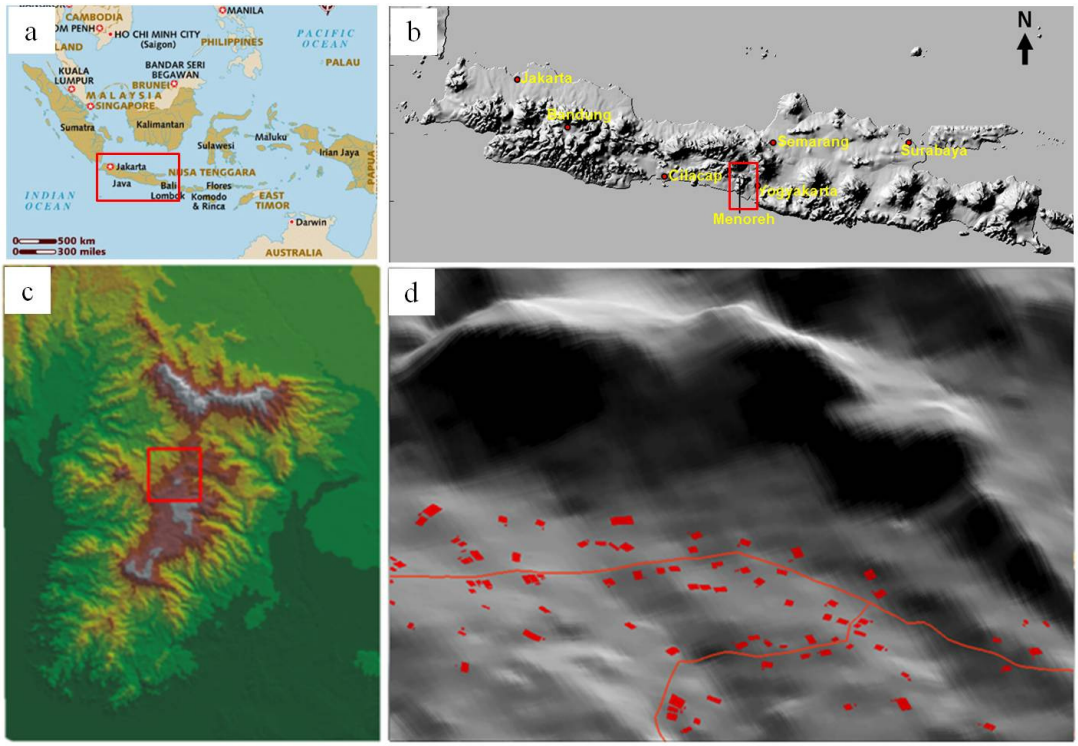

Fig. 1 (a) Map of Indonesia with the red box indicates Java Island (b) Gunung Kelir Area is located in the middle part of Java Island (c) DEM of Menoreh Dome with the red box indicates Gunung Kelir Area (d) 3D view of Gunung Kelir Area with building and main road.

The escarpment is a product of the final uplifting of the Complex West Progo Dome in the Pleistocene[20]. The slope gradient of escarpment varies between 50° and 80°, meanwhile mean of slope gradient is 23.14°. The elevation ranges from 600 to 837.5 m. There are 152 buildings exposed as element at risk in the lower slope of the escarpment.

3. Methodology and Data Collection

3.1 Rockfall Inventory and Frequency-Size

Rockfall inventory is a key issue for frequency-size analysis. Research on rockfall hazard is more challenging in developing country such as Indonesia where no available rockfall catalogue is present. Inventory of rockfall boulder/deposits must be carried on by intensive fieldwork to infer the probability distribution of rockfall size. Recently, several techniques of landslide inventory mapping are developed well, such as aerial photo interpretation[21, 22, 23, 24], surface morphology interpretation of very high resolution DEM[10,25,26 ,27] and interpretation of satellite imagery[28, 29,30]. However, it is rather difficult to be applied in rockfall inventory mapping. For example, the rockfall size in Gunung Kelir area is 31.57 m^3 in average, meaning too small to be interpreted by imagery analysis.. In addition, high density of a canopy layer may reduce the visibility of rockfall boulder below the vegetation layer from imagery data. Thus, extensive geomorphology inventory with transect walk was carried on to plot 521 rockfall boulders in Gunung Kelir area. Coordinate location was recorded by GPS (Global Positioning System) and the size of a boulder was measured by laser rangefinder. Then, all data obtained from fieldwork are transferred into GIS environment.

The temporal probability of rockfall can be inferred from the magnitude-frequency distribution. It was derived from magnitude-cumulative frequency (MCF) curves constructed from rockfall inventory using graphical method[2,13]. Magnitude-cumulative frequency curve was generated by sorting the volume of rockfall and accumulating the incremental frequencies from largest to smallest. It was inferred that the length in years of the total of 521 boulders in the entire area is 141 years. The resulting magnitude-cumulative frequency (MCF) plot is shown in **Fig. 2**.

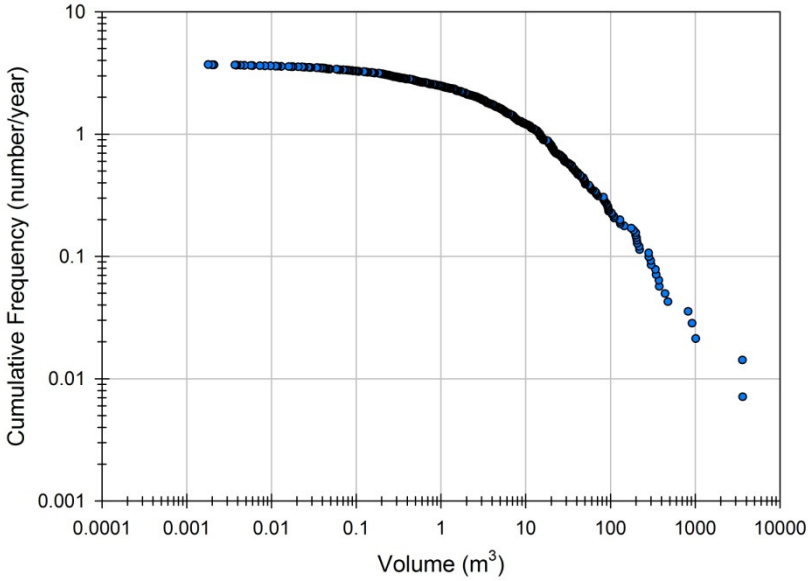

Fig. 2 Magnitude-cumulative Frequency (MCF) Curve

However, the cumulative frequency or incremental frequency is sometime difficult to be employed directly as temporal probability in the hazard analysis. Small volume boulder can have incremental frequency more than 1 (**Fig. 2 and Table 1**). It means that rockfall may occur once or more in each year in a given volume. It does not represent a probability value ranging from 0 to 1. Thus, Poisson probability was employed to calculate the temporal probability of rockfall with the volume in a given volume class.

Table 1 Number of Boulders in each Volume Class in Gunung Kelir Area.

Year = 141	Vol class	Number	Incremental freq.
	<10	352	2.50
	10-100	137	0.97
	100-1000	29	0.21
	>1000	3	0.02

The temporal probability of rockfall was calculated from the observation of the frequency of the past event and MCF relation. It is defined as a percent chance of one or more rockfall in a given volume falling during specified time. It is similar to the hydrology analysis. In this case, rockfalls were treated as recurrent events that occur randomly and independently. Actually, this assumption does not fully accepted because once the rockfall occurs, it may change the slope morphometry which can affect the independency of future events. However, given a certain lack of understanding the physical process on the changing morphometry that control rockfall, Poisson model is one of feasible method to estimate the temporal probability of rockfall events.

There were 16 rockfall events reported by eyewitnesses during 1970-2009 (16 events during period of 39 years) in the lower slope where the total number observed by geomorphological mapping are 58. The rockfall inventory data were collected and documented from field survey which is calculated in the 141-year period (521 rockfall events). The main assumption of temporal probability of rockfall is that rockfall can be considered as independent random point-events in time. The probability of rockfall occurrence during time *t* is:

$$P_N = P[N(t) \geq 1] \tag{1}$$

where N(t) is the number of rockfalls that occur during time *t* in the investigated area.

Probability model is commonly used to investigate the occurrence of independent random point-events in time i.e. Poisson model. The Poisson model considers naturally continuous rockfall data.

$$P[N(t) = n] = \exp(-\lambda t)\frac{(\lambda t)^n}{n!} \qquad n=0,1,2,.... \tag{2}$$

where $P[N(t) = n]$ is the probability of experiencing n landslides during time t, λ is the estimated average rate of occurrence of rockfalls which corresponds to $1/\mu$, with μ is the estimated mean recurrence interval between successive failure events. The variable λ and μ can be obtained from a historical catalogue of landslide events or from a multi-temporal landslide inventory map. The probability of experiencing one or more rockfalls during time t (exceedance probability) as follows:

$$P[N(t) \geq 1] = 1 - P[N(t) = 0] = 1 - \exp^{-\lambda t} \tag{3}$$

$$P[N(t) \geq 1] = 1 - \exp^{\frac{-t}{\mu}} \tag{4}$$

By adopting a Poisson model (eq. 4), the author computed the exceedance probability of having one or more rockfall in each landform (**Table 2**).

3.2 Potential Source Area Identification

The potential rockfall source area was identified by thematic map analysis. Identification of

potential rockfall source was identified by thematic map analysis, e.g. landuse and threshold of slope (**Fig. 3**). Shrub and outcrop are the most potential area being rockfall source, whereas farm/plantation is less potential area being rockfall source. Some farmer plant Teak (Tectona Grandis), Pinus Mercusi, Agathis Alba, Maleleuca sp., and Dalbegia Latifolia in the farm/plantation landuse type. Based on the empirical experience in Gunung Kelir area, slope threshold >55 degree was determined as a potential rockfall source area. The overlay technique of spatial thematic data (e.g. landuse and slope) and analysis of cracking, lithology were employed to determine the potential rockfall area. Once the rockfall trajectory has been simulated, the potential rockfall source was also compared to the boulder deposits obtained from geomorphology inventory.

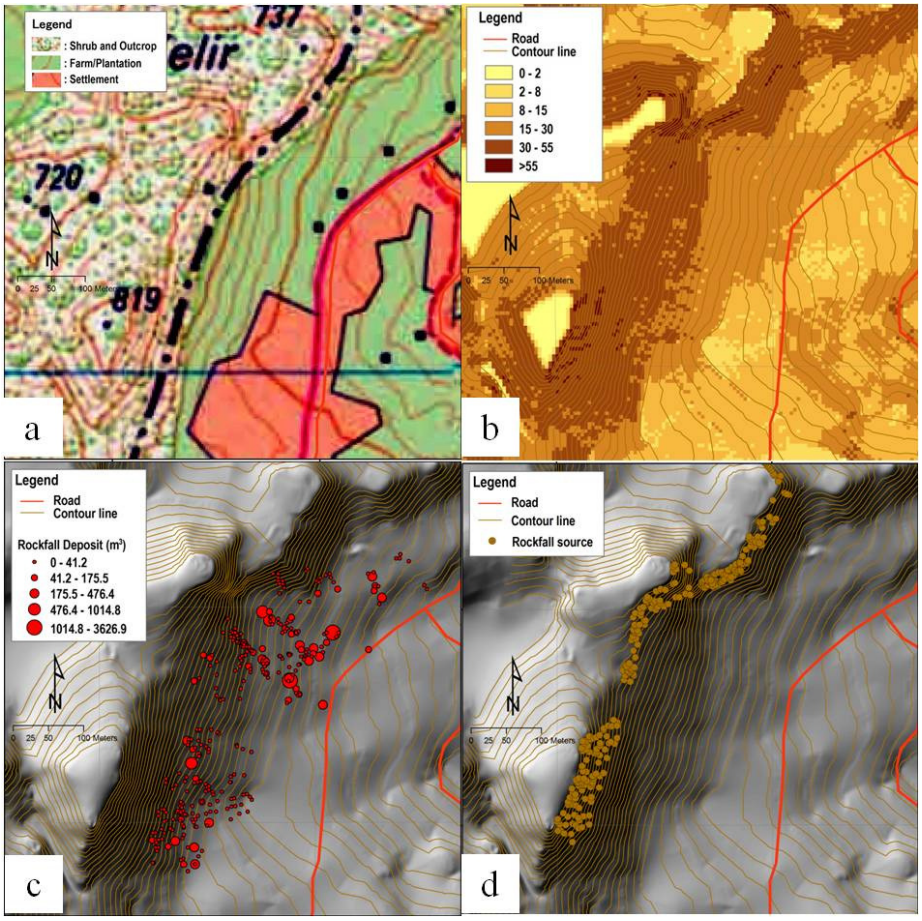

Fig. 3 (a) Landuse Map (b) Slope Map (c) Boulder Deposits from Inventory Mapping (d) Potential Rockfall Source.

3.3 Rockfall Susceptibility Analysis

3.3.1 GIS Rockfall Analyst

GIS modeling based on lumped mass[32] was applied to model the trajectory and velocity of rockfall along the escarpment of Gunung Kelir Indonesia. It considers the dynamic process of rockfall based on the cell plane obtained from raster based Digital Elevation Model (DEM). DEM represents the earth surface or topography containing actual height points. GIS can produce various topographic parameters (derivative of DEM) such as slope, aspect, curvature easily. In GIS

Rockfall analyst, the DEM derivatives, i.e. slope angle and aspect angle are used to construct the normal vector of each cell plane[32]. It is expressed in the global Cartesian system as:

$$u_n = (\sin\theta \sin\varphi, \sin\theta \cos\varphi, \cos\theta) \quad (5)$$

where u_n unit normal vector, θ is the slope angle and φ is the aspect angle.

To reduce the excessive computational requirements in a GIS environment, rockfall analyst employs lumped mass approach to assess the trajectory and velocity of rockfall. It means that the rockfall simulation will not consider the size and shape of the boulder. The rockfall process including the modeling of free falling, bouncing and rolling or sliding is performed by discrete time steps. It is automatically determined by both cell size and particle velocity. Physical quantity of boulder such as rock position, displacement, velocity, acceleration, force and momentum is represented in 3D vector space. For instance, the flying path of boulder computed by parabolic equation is defined as

$$\bar{x} = \begin{bmatrix} 0 \\ 0 \\ -\frac{1}{2}gt^2 \end{bmatrix} + \begin{bmatrix} V_{x0} \\ V_{y0} \\ V_{z0} \end{bmatrix} t + \begin{bmatrix} X_0 \\ Y_0 \\ Z_0 \end{bmatrix} \quad (6)$$

where g is the acceleration due to gravity (9.8 m/s^2), X_0, Y_0, Z_0 is the initial position and V_{x0}, V_{y0}, V_{z0} is the initial velocity of the rock in x, y, z direction. Whereas, the velocity vector of the rockfall is defined as

$$\bar{v} = \begin{bmatrix} V_{x0} \\ V_{y0} \\ V_{z0} - gt \end{bmatrix} = \begin{bmatrix} 0 \\ 0 \\ -gt \end{bmatrix} + \begin{bmatrix} V_{x0} \\ V_{y0} \\ V_{z0} \end{bmatrix} \quad (7)$$

In addition, coefficient restitution is also included to calculate the bouncing velocity in the intersection location between flight path parabola and the grid cell surface. It involves coefficient of normal restitution R_N and coefficient of tangential restitution R_T. The bouncing velocity vector in a local coordinate system is defined as

$$V'_{Dip} = V_{Dip} R_T \quad (8)$$

$$V'_{Trend} = V_{Trend} R_T \quad (9)$$

$$V'_N = V_N R_N \quad (10)$$

where V_{Dip} is the velocity components of rock in the dip direction, V_{Trend} is the velocity components of rock in the trend direction, V_N is the velocity components in normal direction of slope cell. Beside projectile algorithm for falling, the rolling or sliding algorithm is also determined by the interaction between rock velocity vector and the normal vector of cell plane[32].

Table 2 Properties of Surface Material (Adopted from Rocscience website, 2014).

Surface Types	R_N	R_T
Sandstone face	0.53	0.9
Vegetated soil slope	0.28	0.78
Soft soil, some vegetation	0.30	0.3
Limestone face	0.31	0.71
Talus cover with vegetation	0.32	0.8

However, GIS-lumped mass model is dimensionless, meaning that it does not consider the size, shape and fragmentation of the boulder. The more mechanically numerical rockfall simulation is needed as a complementary tool to analyze the trajectory which has a potency of high risk, e.g. trajectory passing a building. It should be able to model the dynamic displacement and deformation

of an elastic body in any shape and consider the rigid body displacement, rotation and deformation of a block. Thus, 2D DDA was employed to confirm the reliable trajectory and dynamic behavior of boulder when travel along the slope having high risk possibility.

3.3.2 2D DDA

Extended 2D DDA[33] was employed to assess the motion behavior of the most dangerous rockfall trajectory obtained from GIS modeling. DDA is one of numerical simulation that can be applied to simulate the motion behavior of rock. It deals with the problem of rigid body movement and large deformation of a rock block system under general loading and boundary[17]. Even though DDA is parallel to finite element, the advantage of 2D DDA is that every single block can be convex or concave in two dimensional polygon. In addition, Coulomb's law is applied to the contact interface and the simultaneous equilibrium equations are solved for each loading or time increment[34]. Each block can interact and deform independently.

There are six displacement variables working in DDA when a block experiences constant stresses and constant strains throughout[35]. The displacement (u,v) of any point (x,y) of a block can be defined as six variables as follows:

$$(u_0\, v_0\, r_0\, \varepsilon_x\, \varepsilon_y\, \gamma_{xy}) \tag{11}$$

where u_0,v_0 are the parallel translation (u,v) of a specific point (x_0,y_0) on the block; r_0 is the rotation angle (in radians) of the block with the rotation center at (x_0,y_0). $\varepsilon_x\, \varepsilon_y\, \gamma_{xy}$ are the normal and shear strains of block at (x_0,y_0). Displacements (u,v) of the point (x,y) containing several mechanisms such as parallel translation, rotation, normal strain and shear strains are formulated separately. Thus, the total displacement (u,v) of the same point (x,y) is the accumulation of displacements induced by six variables (Shi, 1988) . It can be defined as:

$$\begin{bmatrix} u \\ v \end{bmatrix} = \begin{bmatrix} 1 & 0 & -(y-y_0) & (x-x_0) & 0 & (y-y_0) \\ 0 & 0 & (x-x_0) & 0 & (y-y_0) & (x-x_0) \end{bmatrix} \begin{bmatrix} u_0 \\ v_0 \\ r_0 \\ \varepsilon_x \\ \varepsilon_y \\ \gamma_{xy} \end{bmatrix} \tag{12}$$

2D DDA model will take an advantage of a GIS model to simulate the motion behavior of the boulder. 2D slope profile from DEM was imported to the 2D DDA to draw rock block system and to simulate the contact force of multiple falling rock. The displacement behavior of each block in the dynamic simulation can be traced and can be seen at the end of each calculation step.

3.4 Rockfall Hazard Assessment

Hazard in term of landslide is often defined as an estimation of spatial distribution/susceptibility, temporal distribution, size and frequency of landslide which may occur in the future. The information should include the location, size (volume) and velocity of the potential landslides and any resultant detached material and the probability of their occurrence within a given period of time[36]. Rockfall hazard assessment is expected to answer "where", "how frequent" and "how large" rockfall are likely to occur which are not taken into account in landslide susceptibility zoning. However, conducting rockfall hazard assessment that fully complies the rockfall definition is still a challenge and will not be simple to achieve in practice. In this paper, we proposed a methodological framework of rockfall hazard assessment (**Fig. 4**), i.e. identifying the release/potential source, path/trajectories, depositional area, temporal probability, and rockfall intensity. This can bridge the gap between a statistical method which only predict where rockfall will occur in the future based on past inventory and deterministic method which usually analyze rockfall based on simple

mechanical laws and usually applied in limited areas.

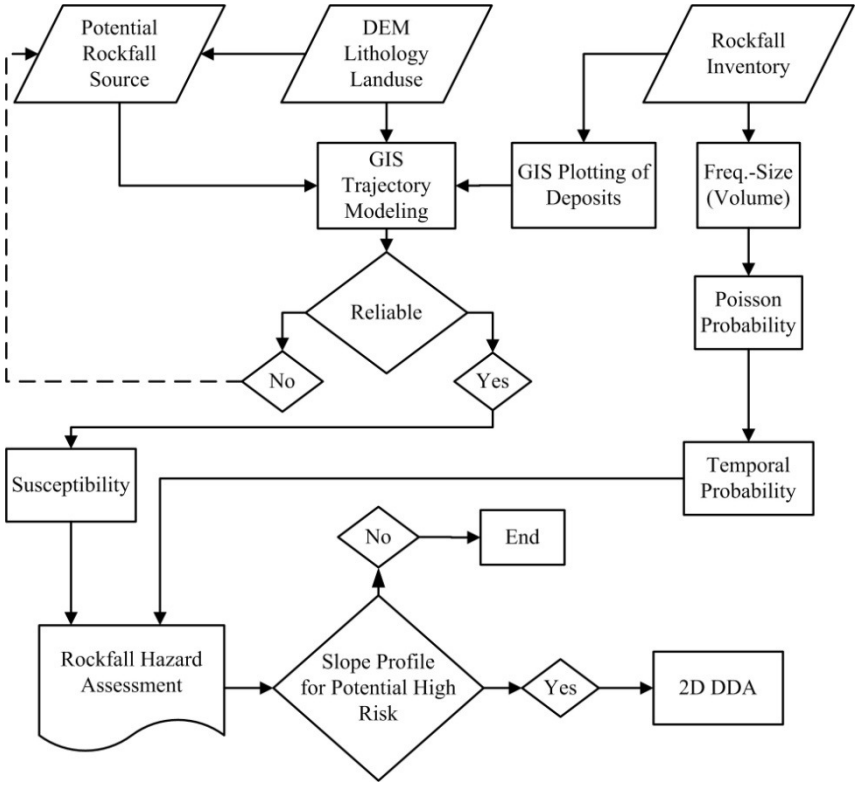

Fig. 4 Methodological Framework of Rockfall Hazard Assessment.

Rockfall hazard (spatial, temporal and magnitude) was defined by integration of geomorphology suvey, statistics and GIS-spatial analysis. Geomorphology survey of rockfall boulders and semi structured interview were conducted to determine the magnitude probability and temporal probability of rockfall. Frequency magnitude analysis of rockfall volume was calculated by observing the cumulative frequency distribution in log-log chart. The size-volume data was used as an input in 2D DDA in order to obtain motion behavior of the most dangerous rockfall trajectory.

The spatial probability of rockfall was described by potential trajectory along the sub-vertical cliff. The result of potential trajectory is controlled by the geomorphology inventory of rock boulder/deposits and spatial analysis of rockfall source. Spatial probability containing the release/potential source, path/trajectories, depositional area has been firstly defined. The most dangerous rockfall trajectory is chosen from the result of the GIS trajectory model. Then, the slope profile of the most dangerous rockfall trajectory and rockfall size distribution are used as input for 2D DDA to compute displacement, rotation and deformation of a block. Thus, the proposed methodological framework does not only provide quantitative input data for the estimation of future risk, but also important for policy making to assist establishment of structural and or nonstructural preventive measures including landuse planning by considering the spatial, temporal and intensity distribution of rockfall occurrence.

4 Results and Discussions

4.1 Temporal Probability

Beside geomorphology inventory, we also conducted semi closed questionnaire interviews to obtain the temporal data of rockfall occurrences. We found that 16 rockfall occurrences have been

observed by eyewitness during 1970-2009. The temporal information was combined with frequency magnitude analysis to obtain probability occurrence of a given volume in a given time period in a given area. The temporal probability is described by the chance one or more rockfall during specified time.

The temporal information applies for hazard assessment in Gunung Kelir. Based on the equation (3) and (4), rockfall in each volume class has a chance of one or more rockfall during a specified time for an area 0.12 km^2. It shows that the smaller volume will have higher chance to occur in a specified time (**Table 3**).

Table 3 Poisson Model for Percent Chance One or more Rockfall on each Volume Class, during Specified Time.

Volume Class	Number per Class	Chance of one or more rockfall during specified time						
		1 yr.	5 yrs.	10 yrs.	25 yrs.	50 yrs.	100 yrs.	141 yrs.
<10	352	0.92	1.00	1.00	1.00	1.00	1.00	1.00
10-100	137	0.62	0.99	1.00	1.00	1.00	1.00	1.00
100-1000	29	0.19	0.64	0.87	0.99	1.00	1.00	1.00
>1000	3	0.02	0.10	0.19	0.41	0.65	0.88	0.95

4.2 Rockfall Hazard in Gunung Kelir

The calculation of GIS rockfall modeling is represented by vector format. It shows trajectories along the escarpment. The starting point of boulder is treated as a seeder location in the convex creep slope. The potential rockfall source area was identified by field survey and thematic map analysis. Sampling distance for seeder along the source area was set as 5 m. The simulation of rock fall trajectory predicts how far a boulder passes through slope. Bouncing, falling, rolling or sliding including the velocity are also able to be investigated in each trajectory. It describes that highest velocity is attained before the end of rock's flight. The potential rockfall source area as polyline seeder were positioned separately based on the pattern of boulder deposition and slope direction. Coefficient of surface parameters (**Table 2**) was also used to control boulder movement during impact at the end of rock flight. The result of trajectory model is also compared to the boulder deposition obtained from GPS plotting and fieldwork activities. The trajectory stop point is good in agreement with the boulder deposition in GIS model.

The rockfall trajectory shows that the northern part and middle part have higher susceptibility than the southern part (**Fig. 5**). There are three buildings potentially obstructed by rockfall. The location of the building is 163 meters from the source of material. The result of the rockfall trajectory model shows that no one of the building is obstructed by rockfall in the southern part. The size of the boulder deposition in the southern part is also relatively small < 20 m^3.

More attention should be prioritized in northern and middle part that can potentially cause building damage. However, the detail of preventive measures development needs more analysis on the mechanic of rockfall process. Thus, 2D DDA was applied to explore the motion behavior of rockfall in the highest potency of high risk. There are 5 materials involved to model the motion behavior of a boulder which has the potential to damage the building in the northern part. The material properties are shown in **Table 4** and control parameter is shown in **Table 5**.

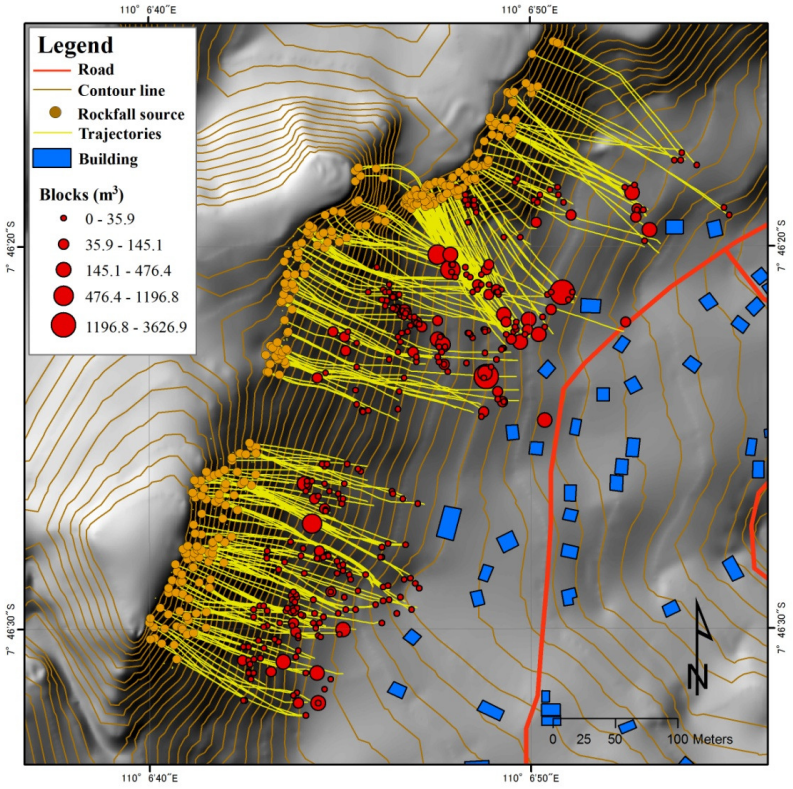

Fig. 5 GIS Rockfall Trajectories.

Table 4 Material properties of Gunung Kelir Rockfall.

	M_1	M_2	M_3	M_4	M_5
Density (ρ): g/cm^3	50000	2500	2450	2500	2450
Unit weight of rock (γ): kN/m^3	0	25	24.5	25	24.5
Elastic modulus (E) : GPa	20	20	20	20	20
Poisson's ratio (v)	0.2	0.2	0.2	0.2	0.2
Friction angle of discontinuities (φ) : °	20	20	30	19	18
Cohesion of discontinuities (c) : MPa	0	0	0	0	0
Tensile strength of discontinuities (σ_t) : kPA	0	0	0	0	0

Table 5 Control Parameters of DDA.

Items	Data
Assumed maximum displacement ratio (g_2)	0.001
Total number of time steps	6000
Time steps (g_1)	0.01
Contact spring stiffness (g_0)	1.0x10^{7}kN/s

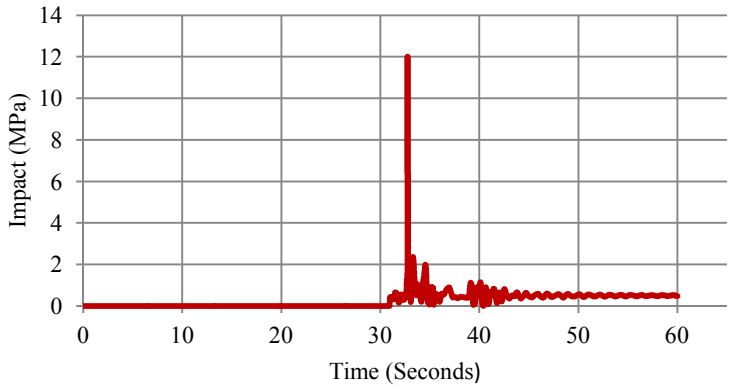

Fig. 6 Rockfall Impact Force.

The result shows that the boulder in the northern part can potentially cause the building damage. The contact between boulder and building was introduced by small boulders with impact force 0.4 MPa at 30.95 seconds. The maximum impact force between boulders and building was 11.9 MPa (32.74 seconds after failure) (**Fig. 6** and **Fig. 7**). It happened before the contact between the big boulder and the building. It was almost 80 times higher compared with the first contact between small boulders and the building. After the maximum impact force, it was followed by contact between medium boulder and the building with the maximum impact force 2.3 MPa in 33.4 seconds. Then, finally the small boulders stoped moving in 43.04 seconds with the impact force around 0.91. The velocity of the boulders is less than 15 m/s. Rolling and sliding are the most common of boulders motion.

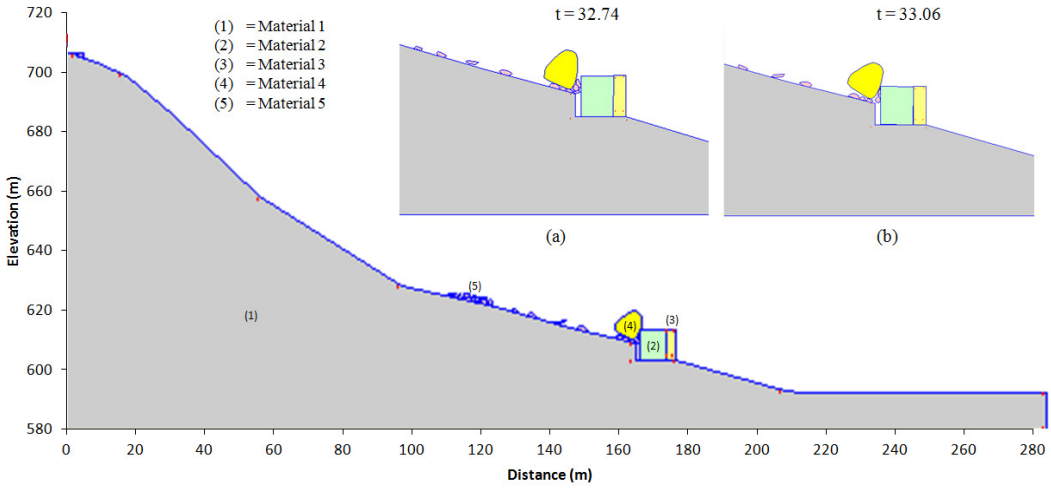

Fig. 7 Rockfall Behaviour for Potential High Risk.

By defining spatial, temporal and intensity distribution of rockfall; structural protection, land planning and or evacuation can be designed effectively. Information of trajectories and deposition is useful for landuse planning. Landuse planning is related to area zoning which needs rockfall information including spatial probability of rockfall hazard, trajectories and final deposition information. Rockfall information can assist policy maker to make zonation on high risk and acceptable risk zone.

In the case of Gunung Kelir area, it is also possible to establish structural preventive measures along the escarpment. However, it is difficult to install structural preventive measures along the escarpment due to limitation of the budget and the socioeconomic condition of Gunung Kelir Area. Thus, the information of trajectories, velocity, impact, and final deposition can assist policy maker to make prioritization for protecting important assets by establishing several scenarios of preventive measures and computing a cost-benefit ratio of applied mitigation technique.

5 Conclusion

Hazard assessment as defined by spatial, temporal and intensity distribution should involve determination of rockfall source, size-frequency, onset susceptibility, temporal probability and deposit area. It represents "where", “how frequent” and “how large” rockfall are likely to occur. GIS-lumped mass rockfall simulation has been employed to identify potential rockfall source based on the distribution of boulders from the past rockfall events. The reliable trajectories can be estimated once the potential rockfall sources were identified. It represents where rockfall is likely to occur called as susceptibility. The rockfall susceptibility shows that the northern part and middle part have higher susceptibility than the southern part and may cause three building damage obstructed by rockfall (potential high risk). More attention should be prioritized on the potential high risk. Since GIS-lumped mass model does not consider the size, shape and fragmentation of the boulder, the more mechanically numerical rockfall simulation is needed as a complementary tool to analyze the trajectory which has a potency of high risk. Thus, 2D DDA was employed to confirm the reliable trajectory and dynamic behavior of boulder when travel along the slope having high risk possibility. Thus, the methodological framework resulting information of rockfall hazard represented as the susceptible location and magnitude-frequency, including temporal probability of rockfall can be further employed to formulate an appropriate landuse plan in a rockfall prone area.

Acknowledgements

The authors would like to acknowledge the funding of Hibah Bersaing DIKTI research grant (contract number UGM/PHB/XVI/2010/1) for field work and data collection.

References

1) O. Hungr and S. G. Evans. Engineering evaluation of fragmental rockfall hazards, Proceedings 5th International Symposium on Landslides, Lausanne, Switzerland, 1, 685–690, (1988).
2) C. Dussauge, J. Grasso, and A. Helmstetter. Statistical analysis of rockfall volume distributions: Implications for rockfall dynamics. Journal of Geophysical Research 108 (2003).
3) G. B. Crosta and F.Agliardi. A methodology for physically based rockfall hazard assessment, Nat. Hazards Earth Syst. Sci., 3,407–422 (2003).
4) D. Peila, C. Oggeri, C. Castiglia. Ground reinforced embankments for rockfall protection: design and evaluation of full scale tests, Landslides 4 : 255-265 (2007).
5) A. Loye, M. Jaboyedoff, A. Pedrazzini. Identification of Potential Rockfall Source areas at regional scale using DEM-based geomorphometric analysis, Nat. Hazards Earth Syst. Sci., 9,1643–1653 (2009).
6) M. Jaboyedoff, and V.Labiouse. Preliminary assessment of rockfall hazard based on GIS data, in: 10th International Congress on Rock Mechanics ISRM 2003 – Technology roadmap for

rock mechanics, South African Institute of Mining and Metallurgy, Johannesburgh, South Africa, 575–578 (2003).

7) F. Guzzetti, P. Reichenbach, and G. F. Wieczorek. Rockfall hazard and risk assessment in the Yosemite Valley, California, USA,Nat. Hazards Earth Syst. Sci., 3, 491–503 (2003).
8) P. Frattini, G. Crosta, A. Carrara, and F. Agliardi. Assessment of rockfall susceptibility by integrating statistical and physicallybased approaches, Geomorphology, 94, 419–437 (2008).
9) H. Aksoy, and M. Ercanoglu. Determination of the rockfall source in an urban settlement area by using a rule-based fuzzy evaluation, Nat. Hazards Earth Syst. Sci., 6, 941–954 (2006).
10) H. Lan, C.D. Martin, C. Zhou, C.H. Lim. Rockfall hazard analysis using LiDAR and spatial modeling. Geomorphology 118 (1–2), 213–223 (2010).
11) D. Santana, J. Corominas, O. Mavrouli, D. Garcia-Selles. Magnitude-frequency relation for rockfall scars using a Terrestrial Laser Scanner. Engineering Geology 145-146 50-64 (2012).
12) G. F. Wieczorek, J. B. Snyder, C. S. Alger, and K. A. Isaacson, Yosemite historical rockfall inventory, U.S Geol. Surv. Open File Rep., 92– 387, 38 pp. (1992).
13) O. Hungr, S. G. Evans, and J. Hazzard, Magnitude and frequency of rock falls along the main transportation corridors of southwestern British Columbia, Can. Geotech. J., 36, 224–238. (1999).
14) C. Dussauge-Peisser, A. Helmstetter, J. R. Grasso, D. Hantz, P. Desvarreux, M. Jeannin, and A. Giraud. Probabilistic approach to rock fall hazard assessment: potential of historical data analysis, Nat. Hazards Earth Syst. Sci. 2, 15–26 (2002).
15) A. Volkwein, K. Schellenberg, V. Labiouse, F. Agliardi, F. Berger, F. Bourrier, L. K. A. Dorren, W. Gerber, M. Jaboyedoff. Rockfall characterisation and structural protection—a review. Nat Hazards Earth Syst 11:2617–2651 (2011).
16) F. Guzzetti, G. Crosta, R. Detti, F. Agliardi. STONE: a computer program for three-dimensional simulation of rock-falls. Computer & Geosciences 28 pp. 1079-1093 (2002).
17) G. Shi. Discontinuous deformation analysis a new numerical model for the static and dynamics of block systems. Ph. D thesis. Berkeley University of California (1988).
18) Winaryo and Sunarto Pengkajian Mitigasi Tanah Longsor Pasca Gempabumi 27 Mei 2006 di Dusun Gunung Kelir, Kecamatan Girimulyo, Kabupaten Kulon Progo DIY. Jurnal Kebencanaan Indonesia (2008).
19) PSBA UGM. Penyusunan Sistem Informasi Penanggulangan Bencana Tanah Longsor di Kabupaten Kulon Progo. UGM (2008).
20) R.W. van Bemmelen. The Geology of Indonesia, Vol II., GovernmentPrinting Office the Hague (1949).
21) M. Cardinali, F. Guzzetti, E.E. Brabb. Preliminary map showing landslide deposits and related features in New Mexico. U.S. Geological Survey Open File Report 90/293, 4 sheets, scale 1:500,000 (1990).
22) F. Brardinoni, O. Slaymaker, M.A. Hassan. Landslide inventory in a rugged forested watershed: a comparison between air-photo and field survey data. Geomorphology 54 (3–4), 179–196 (2003).
23) T.Y. Duman, T. Çan, Ö. Emre, M. Keçer, A. Doğan, A. Şerafettin, D. Serap. Landslide inventory of northwestern Anatolia, Turkey. Engineering Geology 77(1–2), 99–114 (2005).
24) F. Fiorucci, M. Cardinali, R. Carlà, M. Rossi, A.C. Mondini, L. Santurri, F. Ardizzone, F. Guzzetti. Seasonal landslides mapping and estimation of landslide mobilization rates using aerial and satellite images. Geomorphology 129 (1–2), 59–70 (2011).

25) W.H. Schulz. Landslides Mapped using LIDAR Imagery, Seattle, Washington. U.S. Geological Survey Open-File Report 2004-1396 (2004).
26) M.H. Derron and M. Jaboyedoff. Preface to the special issue: LIDAR and DEM techniques for landslides monitoring and characterization. Natural Hazards and Earth System Sciences 10 (9), 1877–1879 (2010).
27) K.A. Razak, M.W. Straatsma, C.J. van Westen, J.-P. Malet, S.M. de Jong.. Airborne laser scanning of forested landslides characterization: terrain model quality and visualization. Geomorphology 126, 186–200. (2011).
28) J. Barlow, S. Franklin, Y. Martin. High spatial resolution satellite imagery, DEM derivatives, and image segmentation for the detection of mass wasting processes. Photogrammetric Engineering and Remote Sensing 72, 687–692 (2006).
29) A.M. Borghuis, K. Chang, H.Y. Lee. Comparison between automated and manual mapping of typhoon-triggered landslides from SPOT-5 imagery. International Journal of Remote Sensing 28, 1843–1856 (2007).
30) Z. Ren and A. Lin. Co-seismic landslides induced by the Wenchuan Mw 7.9 earthquake, revealed by ALOS PRISM and AVNIR2 imagery data. International Journal of Remote Sensing 31, 3479–3493 (2010).
31) J. R.Taylor. An Introduction to Error Analysis, 2nd Ed., 327 pp., Univ. Sci. Books, Sausalito, Calif. (1997).
32) H. Lan, C. D. Martin, and C. H. Lim. RockFall analyst: a GIS extension for three-dimensional and spatially distributed rockfall hazard modelling, Computer and Geoscience., 33, 262–279 (2007).
33) G. Chen. Numerical Modelling of Rockfall using Extended DDA. Chinese Journal of Rock Mechanics and Engineering, 22 (6):926-931 (2003).
34) G. Shi and R. E. Goodman. Generalization of Two-Dimensional Discontinuous Deformation Analysis for Forward Modelling. International Journal for Numerical and Analytical Methods in Geomechanics, vol. 13, pp. 359-380 (1989).
35) G. Shi and R. E. Goodman. Two dimensional Discontinuous Deformation Analysis. International Journal for Numerical and Analytical Methods in Geomechanics, vol. 9, pp. 541-556 (1985).
36) Joint Technical Committee on Landslide and Engineered Slope (JTC-1). Guidelines for Landslide Susceptibility, Hazard and Risk Zoning for Landuse Planning. Engineering Geology 103, 85-98 (2008).